Event-Triggered Controller Design for Multi-Agent Systems

Zeyuan Wang and Mohammed Chadli, University of Paris-Saclay, IBISC Laboratory, Evry, France

Abstract

This chapter presents an event-triggered controller design for multi-agent systems, where the data transmission among agents is governed by event-triggered mechanisms. The dynamic event-triggered control with the full-state observer is introduced, with a particular concern of reducing communication frequency through designable inter-event time. An extension to directed topology, where the communication is restricted to single directions, is also discussed. The proposed methods follow the co-design principle, where the parameters of controllers, observers, and event-triggered mechanisms are synthesized simultaneously. Following a distributed design principle, only local information is required in a small range of nearby neighbors to compute the control signal and the event-triggered condition. Zeno behavior is proved to be excluded. Finally, the proposed approaches are demonstrated by a numerical example and compared with other methods to validate their effectiveness.

Key Points

- In this chapter, a systematic approach for designing dynamic event-triggered controllers for generic linear multi-agent systems is introduced, focusing on minimizing communication times. Following a co-design process, the results incorporate a distributed controller and observer synthesis, which are formulated by the linear matrix inequality approach.
- Different assumptions are discussed, including scenarios of undirected topology and directed topology, where the latter is a more general case with directed communication and unbalanced graphs.
- The proposed methods adopt a distributed design process, demonstrating that only local information is required to generate control signals and determine event-triggering conditions, which can serve as a design reference for practical engineering.

Chapter Introduction

This chapter presents methods of designing event-triggered controllers for multi-agent systems. Starting with an introduction to multi-agent technology and event-triggered control, this chapter presents a design process for event-triggered communication mechanisms with distributed controllers and distributed observers, with a particular focus on reducing communication frequency. The presented methods follow the co-design principles, wherein the gains of the controller and parameters of the event-triggered mechanism are simultaneously designed, as opposed to emulation-based approaches. The linear matrix inequalities approach is employed for the synthesis of controllers and observers. Numerical simulation is illustrated at the end of the chapter.

Introduction

Before proceeding with this chapter, some background research, including the current state of multi-agent systems and event-triggered control, is introduced.

 doi:10.1016/B978-0-443-14081-5.00124-0

Multi-Agent Systems

The research of multi-agent systems (MASs) emerged in the 1980s, experienced significant development in the mid-1990s, and has since evolved into an essential aspect of distributed artificial intelligence. MASs comprise autonomous agents interacting with each other to achieve common objectives. These agents exhibit autonomy, learning capabilities, and decision-making processes. The advancements in technology have highlighted the importance of MASs. These systems have a wide range of applications, from coordinating unmanned aerial vehicles to underwater cooperation and robot formation control. With such diverse applications, it is crucial to address the cooperative control issues within MASs.

In recent years, diverse consensus mechanisms have been explored within MASs, including leaderless consensus and leader-following consensus. Leaderless consensus focuses on achieving agreement among agents without a designated leader, while leader-following consensus involves consensus with specified leader agents, which is the focus of this chapter (also known as the model reference consensus (Vazquez Trejo *et al.*, 2020)). This topic has been extensively explored for linear MASs (Ni and Cheng, 2010; Yang *et al.*, 2022), nonlinear MASs (Han *et al.*, 2022), and scenarios involving homogeneous or heterogeneous agents (Guo *et al.*, 2023). Techniques employed for leader-following consensus can also be extended to address challenges in formation control (Ge and Han, 2017), which is also an important application of MASs.

Consensus control in MASs can be achieved through centralized control, decentralized control, or distributed control. Centralized control involves a single entity computing control signals for all agents (Dimarogonas *et al.*, 2012), while decentralized control distributes this process among agents, which use only their own information (Yang *et al.*, 2016). Distributed control allows agents to make decisions based on local information from itself and its nearby neighbors, enabling autonomy and adaptability (Fan *et al.*, 2013). This distributed control paradigm will be employed in this section.

Recent research has also studied the impact of constraints on MASs, such as fault-tolerance control (Trejo *et al.*, 2022; Wang and Chadli, 2024c; Wang and Chadli, 2024b), noise resilience (Hanada *et al.*, 2023), and time-varying delays (Wang *et al.*, 2022). The complex network environment of MASs has also been addressed in the context of cyberattacks (Wen *et al.*, 2023) and switching topology (Gu *et al.*, 2023), showcasing the field's ability to adapt to contemporary challenges. One of the major challenges in MASs is event-triggered control/communication, where decisions and communications are based on pre-designed event rules instead of continuous or periodical sampling. This approach aims to optimize resource utilization and reduce communication frequency in MASs.

Event-Triggered Control for Multi-Agent Systems

The traditional time-triggered control in MASs raises challenges of high network burden, more resource consumption, and more energy limitations (Qiu *et al.*, 2019). The periodic control updates and data transmissions in time-triggered systems may lead to inefficiencies and increased demands on communication networks and computing resources. To address these issues, researchers have turned to event-triggered mechanisms (ETMs), which offer a more adaptive approach to governing communication and control updates. Large-scale MASs can benefit from ETMs that minimize data sampling, communication, and control updates while maintaining system performance. Unlike time-triggered systems, ETMs operate based on events, where triggering conditions are the core component for controlling when a control update or data transmission should occur. This allows agents to avoid unnecessary communication.

The concept of ETM for stabilization control can be traced back to the work of Tabuada (2007). Since then, ETM has undergone significant development and has found applications in various dynamic systems (Qi *et al.*, 2023; Wu *et al.*, 2023), in leaderless consensus problems (Dimarogonas *et al.*, 2012), and its subsequent adaptation for second-order linear MASs (Chen and Hao, 2015). Recent advancements in ETM include the development of distributed control in MASs. For example, Li *et al.* (2020) proposes an adaptive fully distributed event-triggered/self-triggered control, addressing the challenges posed by external disturbances. In Cheng and Li (2019), an edge-based distributed ETM is introduced for coordinated tracking problems, while Xu *et al.* (2022) presents an observer-based fully distributed ETM that does not require prior knowledge of global information. In the design of ETMs, Zeno behavior is an important issue, which occurs when an infinite number of events happen in a finite time. Therefore, it is essential and necessary to guarantee that Zeno behavior is excluded.

To further reduce communication times in traditional ETM, a dynamic event-triggered mechanism (DETM) was introduced in Girard's work in 2015 (Girard, 2015) proposing a new method to increase the inter-event time (IET). The DETM introduces auxiliary dynamic variables (ADVs) to make event-triggering decisions more intelligent, resulting in lower sampling rates (Ge *et al.*, 2021). In Yang *et al.* (2023), a DETM is designed to handle both reliable and unreliable communication scenarios, considering uncertainties associated with denial-of-service attacks. Additionally, Hou and Dong (2023) proposes a robust adaptive DETM to address challenges related to actuator faults and external disturbances. Moreover, DETM has been applied to various practical scenarios, including formation control (Ge and Han, 2017) and leader-following control (Meng *et al.*, 2023). A more comprehensive survey of ETMs for MASs can be found in Nowzari *et al.* (2019).

However, the adjustment of the IET or minimum IET (MIET) raises practical challenges in implementation. The tuning methods of MIET often involve multiple design parameters and complex relationships between MIET and system parameters (Shi, 2021; Wu *et al.*, 2018). In Berneburg and Nowzari (2019) and Wu *et al.* (2022), ADVs are designed as clock-like variables, providing more flexibility in selecting a preferred MIET. The tuning method involves only the upper bound of the ADV, represented as a scalar. Increasing this parameter can extend the MIET while still guaranteeing the consensus. However, it is essential to

note that a longer IET might sacrifice some convergence performance and that the transient behavior could be degraded. Typically, the compromise of transient performance loss is deemed acceptable. The idea of Berneburg and Nowzari (2019) is also well implemented in Chu *et al.* (2020) for single nonlinear systems without consideration of the state observer and is also extended in Wang and Chadli (2023b) and Wang and Chadli (2023c) by a moving average approach. In the work presented by Zhang *et al.* (2023), the designable MIET is achieved using the parametric Lyapunov equation. This approach is not limited to ETC but extends to self-triggered control, with Zeno behavior proven to be excluded. Additionally, in the work of Li *et al.* (2023), the MIET is designed through the proposed DETM under the constraint of input saturation.

In some literature, MASs equipped with ETMs can also be modeled as hybrid systems. A hybrid system incorporates an additional set of discrete state equations. The system's continuous states satisfy a set of continuous-time differential equations (i.e., the state is in the flow set), and when the triggering function is activated (i.e., the state is in the jump set), the state is represented through a jump map. Consequently, control systems can utilize some existing conclusions and methods from hybrid systems. The scope of this chapter does not cover designing ETMs from the view of hybrid systems; interested readers may refer to literature such as Liu *et al.* (2021), Donkers and Heemels (2012) and Borgers and Heemels (2014) for further information.

Outline

In the rest of the chapter, methods for designing event-triggered controllers in MAS are introduced, focusing on reducing communication frequency using DETMs. In Section "Distributed Observer-Based Dynamic Event-Triggered Control for Multi-Agent Systems", a general design framework of DETM with distributed observers and adjustable MIET is introduced, including the case of undirected and directed topologies. The design conditions are formulated by matrix inequalities, followed by linearization methods under certain assumptions. The exclusion of Zeno behavior is also guaranteed. Section "Numerical Example" demonstrates the effectiveness of the theoretical methods through a numerical example. The chapter ends with conclusions and perspectives in Section "Conclusion and Perspective".

Distributed Observer-Based Dynamic Event-Triggered Control for Multi-Agent Systems

Most above-mentioned ETM or DETM assume that the states of agents are all measurable, such as in Zhang *et al.* (2023), Li *et al.* (2023), Berneburg and Nowzari (2019), Wu *et al.* (2022), Hou and Dong (2023) and Chu *et al.* (2020). However, this assumption is still far from reality, and the internal state is not always available in application. One of the solutions is to design state observers. Unlike the single system, observers for MASs entail a co-design problem that involves event-triggered control and estimation. Some studies have addressed this issue. Indeed, in Zhang *et al.* (2014), the controller/observer co-design problem for generic linear MASs to handle leaderless consensus is studied. The results are further developed in Hu *et al.* (2015) for the leader-following problem but only apply to second-order linear MASs. In Zhu *et al.* (2022), an observer-based ETM is proposed to deal with formation control problems under switching and directed topology. A more generic approach is proposed in Trejo *et al.* (2022), which uses linear matrix inequalities (LMIs) to synthesize the controller and observer, but the final strategy is not distributed. The aforementioned studies are based on static ETMs, while few utilize DETMs. Notably, Pham and Nguyen (2023) and Ruan *et al.* (2020) design observers-based DETM while also eliminating the Zeno behavior. However, the complexity of parameter tuning presents a challenge when designing the MIET. Based on the above discussion, synthesizing a distributed controller and observer under DETM with adjustable MIET has yet to be fully explored.

In this section, the DETM for MAS control is designed with adjustable MIET, and the sequel presents an extension of the results for directed topology, which allows for directed communication.

Notations Given a matrix P, P^T denotes its transpose. If P is a square matrix, $\lambda_{min}(P)$ and $\lambda_{max}(P)$ denote the minimum and maximum eigenvalues of P respectively, and P^{-1} represents its inverse. Denote $P^{-T} = (P^T)^{-1}$ $P<0(\leq 0)$ denotes that P is negative definite (negative semi-definite), and $P>0(\geq 0)$ means $-P<0(\leq 0)$. Denote I_n an n-dimensional identity matrix. $\otimes$ is the Kronecker product. $\|\cdot\|$ is the ℓ_2-norm for a vector or the spectrum norm for a matrix. Define $\mathrm{He}(P) = P + P^T$.

The communication topology of N follower agents is represented by a weighted graph $\mathcal{G} = (\mathcal{V}, \mathcal{E})$, with a vertex set $\mathcal{V} = \{v_1, \ldots, v_N\}$ and an edge set $\mathcal{E} \subseteq \mathcal{V} \bar{n} \mathcal{V}$. The follower agent i and the leader agent are represented as vertices v_i and v_0, respectively. Denote $\mathcal{N}_i$ the set of neighbors of agent i.Define the weighted adjacency matrix $\mathcal{A} = (a_{ij}) \in \mathbb{R}^{N \bar{n} N}$ of $\mathcal{G}$ as $a_{ii} = 0$, $a_{ij} = 1$ if v_i is connected to v_j (i.e., there exists a directed edge (v_i, v_j) from v_j to v_i) and $a_{ij} = 0$ otherwise. If $a_{ij} = a_{ji}$ for any (i, j), then the graph is undirected. Otherwise, it is directed, i.e., a digraph. Define the Laplacian matrix $\mathcal{L} = (l_{ij}) \in \mathbb{R}^{N \bar{n} N}$ as $l_{ij} = -a_{ij}, i \neq j$ and $l_{ii} = \sum_{i \neq j} a_{ij}$. Define $\overline{\mathcal{G}} = (\overline{\mathcal{V}}, \overline{\mathcal{E}})$ as the augmented graph of $\mathcal{G}$, with $\overline{\mathcal{V}} = \mathcal{V} \cup \{v_0\}$ and $\overline{\mathcal{E}} = \mathcal{E} \cup \Delta \mathcal{E}$, where $(v_i, v_0) \in \Delta \mathcal{E}$ if agent i is connected to the leader. Define $\mathcal{D} = diag(d_1, \ldots, d_N)$ as a diagonal matrix where its diagonal element $d_i > 0$ if $(v_i, v_0) \in \overline{\mathcal{E}}$ otherwise $d_i = 0$. Define $\mathcal{H} = \mathcal{L} + \mathcal{D}$.

Problem Statement

The MAS in this chapter is characterized by general linear systems with N follower agents and one leader, represented in the following equations

$$\begin{cases} \dot{x}_i(t) & = Ax_i(t) + Bu_i(t), \ \ y_i(t) = Cx_i(t), \ \ i = 1,\ldots,N \\ \dot{x}_0(t) & = Ax_0(t) \end{cases} \tag{1}$$

where $x_i(t)$ is follower agents' state and $x_0(t)$ is the leader's state. $A \in \mathbb{R}^{n\tilde{n}n}, B \in \mathbb{R}^{n\tilde{n}m}$, $u_i(t) \in \mathbb{R}^m$ is the control input. Define the consensus error of agent i as $\varepsilon_i(t) = x_i(t) - x_0(t)$ and $\varepsilon(t) = \left[\varepsilon_i^T(t), \ldots, \varepsilon_N^T(t)\right]^T$. In order to estimate agents' internal states, Luenberger-type observers are designed for each follower agent i to reconstruct the state $x_i(t)$ from the output $y_i(t)$ and the input $u_i(t)$:

$$\begin{cases} \dot{\tilde{x}}_i(t) & = A\tilde{x}_i(t) + Bu_i(t) + L_o(\tilde{y}_i(t) - y_i(t)) \\ \tilde{y}_i(t) & = C\tilde{x}_i(t) \end{cases} \tag{2}$$

where $L_o \in \mathbb{R}^{n\tilde{n}r}$, and $\tilde{x}_i(t)$ is the observer state. Define observer error of agent i as $\zeta_i(t) = \tilde{x}_i(t) - x_i(t)$ and $\zeta(t) = \left[\zeta_1^T(t), \ldots, \zeta_N^T(t)\right]^T$.

The proposed event-triggered control input $u_i(t)$ of agent i is defined as

$$\begin{cases} u_i(t) = Kz_i(t) \\ z_i(t) = \sum\limits_{j \in \mathcal{N}_i} a_{ij}(\hat{x}_j(t) - \hat{x}_i(t)) + d_i(x_0(t) - \hat{x}_i(t)) \end{cases} \tag{3}$$

where $K \in \mathbb{R}^{m\tilde{n}n}$ is the gain of the feedback control. $\hat{x}_i(t) \ \ i \in 1, \ldots, \mathrm{N}\}$ is the event-generated state which is defined as:

$$\hat{x}_i(t) = e^{A(t-t_k^i)}\tilde{x}_i(t_k^i), \ \ t \in [t_k^i, t_{k+1}^i) \tag{4}$$

where $\tilde{x}_i(t_k^i)$ is the observer state at the last triggering moment t_k^i, and t_{k+1}^i is defined by event-triggered rules given in following sections. Define measurement error of agent i as $e_i(t) = \hat{x}_i(t) - \tilde{x}_i(t)$ and $e(t) = \left[e_1^T(t), \ldots, e_N^T(t)\right]^T$. Note that in practical engineering, the leader is usually specially chosen or a reference model, which can be treated independently. Therefore, it is reasonable to assume that its state is known, i.e., $\hat{x}_0(t) = \tilde{x}_0(t) = x_0(t)$.

The objective is to design an event-triggered mechanism to determine the triggering moment t_k^i under the control law (3).

The data transmission process of agent i ($i \in 1, \ldots \mathrm{N}\}$) is presented in **Fig. 1** and is described as follows: At the triggering moment t_k^i, agent i transmits its current estimated state $\tilde{x}_i(t_k^i)$ to its neighbors. Simultaneously, agent i updates the value of $\hat{x}_i(t_k^i)$ to $\tilde{x}_i(t_k^i)$, thus updating the control input in (3). When agent i receives the value of $\tilde{x}_j(t)$ from a neighbor agent j at the neighbor's triggering moments $t = t_{k'}^j$, the value of $\hat{x}_j(t_{k'}^j)$ in (3) is also updated to $\tilde{x}_j(t_{k'}^j)$.

The following assumptions are considered in this section:

Assumption 1 *The pair* (A, B) *is stabilizable, and the pair* (A, C) is observable.

Assumption 2 *The graph* $\mathcal{G}$ *is weighted, undirected, and fixed.*

Assumption 3 *The augmented graph* $\overline{\mathcal{G}}$ *contains a spanning tree with the leader agent being its root.*

By definition, one can deduce that $\hat{x}_i(t) = e_i(t) + \tilde{x}_i(t)$, $x_i(t) = x_0(t) + \varepsilon_i(t)$, and $\tilde{x}_i(t) = \zeta_i(t) + x_i(t)$, then it follows that

$$z_i = \ \ \sum_{j \in \mathcal{N}_i} a_{ij}(e_j - e_i + \varepsilon_j - \varepsilon_i + \zeta_j - \zeta_i) + d_i(-e_i - \varepsilon_i - \zeta_i) \tag{5}$$

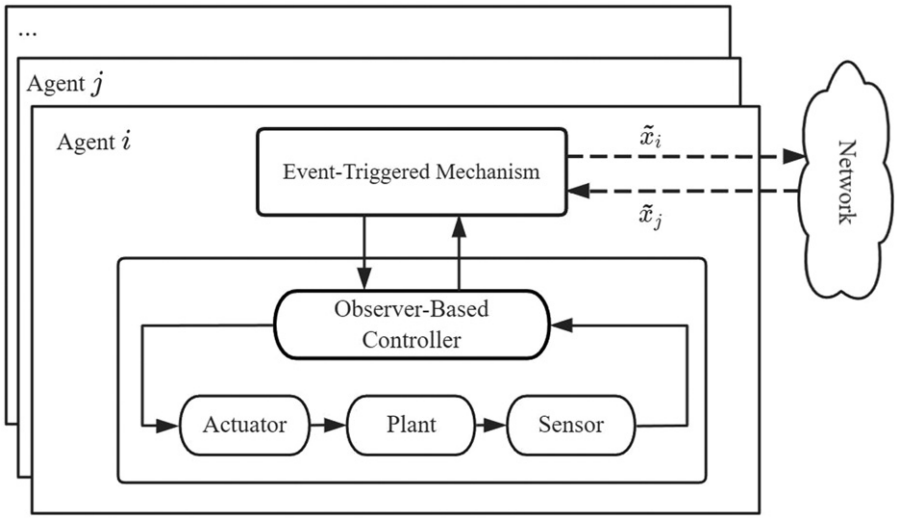

Fig. 1 The event-triggered mechanism.

Define $z(t)=\left[z_1^T(t),\ldots,z_N^T(t)\right]^T$, it follows that

$$z=-(\mathcal{L}\otimes I_n)(e+\varepsilon+\zeta)-(\mathcal{D}\otimes I_n)(e+\varepsilon+\zeta)=-(\mathcal{H}\otimes I_n)(e+\varepsilon+\zeta) \tag{6}$$

By calculating the derivatives of $\varepsilon(t)$, $\zeta(t)$, and $e(t)$, one can obtain the dynamic of the error system:

$$\begin{cases}\dot{\varepsilon}= & (I_N\otimes A-\mathcal{H}\otimes BK)\varepsilon-(\mathcal{H}\otimes BK)(\zeta+e)\\ \dot{\zeta}= & (I_N\otimes(A+L_oC))\zeta\\ \dot{e}= & (\mathcal{H}\otimes BK)\varepsilon+(I_N\otimes A+\mathcal{H}\otimes BK)e+(\mathcal{H}\otimes BK-I_N\otimes L_oC)\zeta\end{cases} \tag{7}$$

By this transformation, the leader-following consensus of the MAS (1) is equivalent to studying the stability of the error system (7).

Dynamic Event-Triggered Mechanism With Adjustable Minimum Inter-Event Time

This section presents a method of synthesizing the proposed controller and the DETM. The DETM design for distributed MAS control is presented in the following theorem.

Theorem 1 (Wang and Chadli, 2024a) *The MAS described in (1) will achieve leader-following consensus under the control law defined in (3) if the following bilinear matrix inequalities (BMIs) are satisfied with regard to* $P_1>0$, $P_2>0$, the controller gain K, and the observer gain L_o:

$$S=\begin{pmatrix}I_N\otimes \mathrm{He}(P_1A)-\mathcal{H}\otimes \mathrm{He}(P_1BK) & -\mathcal{H}\otimes(P_1BK)\\ * & I_N\otimes \mathrm{He}(P_2A+P_2L_oC)+(b_1+b_2)I_{Nn}\end{pmatrix}<0 \tag{8}$$

with positive scalars b_1,b_2, and the event-triggered rule of agent i is defined as

$$\begin{aligned}t_{k+1}^i &\triangleq inf\left\{t>t_k^i|\theta_i(t)\leq 0\right\},\theta_i(t_k^i)=\overline{\theta}_i\\ \dot{\theta}_i(t) &=\begin{cases}min(\omega_i(t),0)-\tau_i, & \text{if}\|e_i(t)\|\neq 0\\ -\tau_i, \text{ otherwise}\end{cases},\ t\in[t_k^i,t_{k+1}^i)\end{aligned} \tag{9}$$

where $\overline{\theta}_i$ and τ_i are arbitrary positive constants, and $\omega_i(t)$ is defined as:

$$\omega_i(t)\triangleq -\frac{e_i^TQe_i}{e_i^TP_3e_i}-\frac{\varepsilon\left(\frac{1}{k}-\frac{1}{2\delta_{max}^2}\right)}{e_i^TP_3e_i}\|z_i\|^2-\frac{e_i^T(2M_1-2\theta_iM_3)z_i}{e_i^TP_3e_i} \tag{10}$$

where

$$\begin{cases}Q=\left(\frac{\varepsilon k}{\delta_{min}^2}-\frac{\varepsilon}{2}+2\delta_{max}\|M_1\|\right)I_n+2\theta_iP_3A+\frac{\delta_{max}^2}{b_1}M_1^TM_1+\frac{\theta_i^2}{b_2}M_2^TM_2\\ M_1=K^TB^TP_1,M_2=P_3L_oC,M_3=P_3BK\end{cases} \tag{11}$$

and $\delta_{min}=\lambda_{min}(\mathcal{H})$, $\delta_{max}=\lambda_{max}(\mathcal{H})$, $k>2\delta_{max}^2$, $P_3>0$. ε is a positive scalar satisfying $S+\varepsilon I\leq 0$.

Proof. The proof consists of showing the stability of the closed-loop system (7) by the Lyapunov theorem. Choose the following Lyapunov function $V(t)$:

$$\begin{cases}V(t)=V_1(t)+V_2(t)+V_3(t)\\ V_1(t)=\varepsilon(t)^T(I_N\otimes P_1)\varepsilon(t),V_2(t)=\zeta(t)^T(I_N\otimes P_2)\zeta(t),V_3(t)=e(t)^T(\Theta(t)\otimes P_3)e(t)\end{cases} \tag{12}$$

where $P_1,P_2,P_3>0$, $\Theta(t)=\mathrm{diag}(\theta_1(t),\ldots,\theta_N(t))>0$, and $\dot{\Theta}(t)<0$ by definition of event-triggered rule (9), thus $V(t)\geq 0$. The derivatives of V_1,V_2,V_3 along the system trajectory are

$$\begin{cases}\dot{V}_1=2\varepsilon^T(I_N\otimes P_1A-\mathcal{H}\otimes M_1^T)\varepsilon-2\varepsilon^T(\mathcal{H}\otimes M_1^T)e-2\varepsilon^T(\mathcal{H}\otimes M_1^T)\zeta\\ \dot{V}_2=2\zeta^T(I_N\otimes P_2(A+L_oC))\zeta\\ \dot{V}_3=2e^T(\Theta\otimes P_3A+\Theta\mathcal{H}\otimes M_3)e+2e^T(\Theta\mathcal{H}\otimes M_3)\varepsilon+e^T(\dot{\Theta}\otimes P_3)e+2e^T(\Theta\mathcal{H}\otimes M_3-\Theta\otimes M_2)\zeta\end{cases} \tag{13}$$

Notice that the matrix $\mathcal{H}$ is positive definite and invertible, thus $\varepsilon=-(\mathcal{H}^{-1}\otimes I)z-e-\zeta$. The Cauchy-Schwarz inequality holds:

$$2e^T(\mathcal{H}\otimes M_1-\Theta\otimes M_2)\zeta\leq\frac{1}{b_1}e^T(\mathcal{H}^2\otimes M_1^TM_1)e+\frac{1}{b_2}e^T(\Theta^2\otimes M_2^TM_2)e+(b_1+b_2)\zeta^T\zeta \tag{14}$$

where $b_1,b_2>0$, then by (13) one can obtain

$$\begin{aligned}\dot{V}=&2\varepsilon^T(I_N\otimes P_1A-\mathcal{H}\otimes M_1^T)\varepsilon-2\varepsilon^T(\mathcal{H}\otimes M_1^T)\zeta+2\zeta^T(I_N\otimes P_2(A+L_oC))\zeta+(b_1+b_2)\zeta^T\zeta\\ &+e^T\left(\frac{\mathcal{H}^2}{b_1}\otimes M_1^TM_1+\frac{\Theta^2}{b_2}\otimes M_2^TM_2\right)e-2e^T(\Theta\otimes M_3-I_N\otimes M_1)z+2e^T(\Theta\otimes P_3A+\mathcal{H}\otimes M_1)e\\ &+e^T(\dot{\Theta}\otimes P_3)e\end{aligned} \tag{15}$$

The first four terms in (15): $2\varepsilon^T(I_N\otimes P_1A-\mathcal{H}\otimes M_1^T)\varepsilon-2\varepsilon^T(\mathcal{H}\otimes M_1^T)\zeta+2\zeta^T(I_N\otimes P_2(A+L_oC))\zeta+(b_1+b_2)\zeta^T\zeta$ form a quadratic expression with regard to ε and ζ, which could be written as $\delta^TS\delta$, with $\delta=(\varepsilon^T\ \ \zeta^T)^T$ and S defined in (8). Since $S+\epsilon I\leq 0$, one can have $\delta^TS\delta\leq-\varepsilon\|\delta\|^2=-\varepsilon(\|\varepsilon\|^2+\|\zeta\|^2)$. And notice that

$$-\varepsilon(\|\varepsilon\|^2+\|\zeta\|^2)\leq-\varepsilon(\varepsilon+\zeta)^T(\varepsilon+\zeta)/2 \tag{16}$$

For the sake of brevity, let $\mathcal{H}^{-2}$ denote $\left(\mathcal{H}^{-1}\right)^2$. Substituting $z=-(\mathcal{H}\otimes I)(\varepsilon+\zeta+e)\Rightarrow\varepsilon+\zeta=-(\mathcal{H}^{-1}\otimes I)z-e$ in (16), and use the fact that $\delta_{max}^{-2}I\leq\mathcal{H}^{-2}\leq\delta_{min}^{-2}I$, one can obtain

$$-\varepsilon\left(\|\varepsilon\|^2+\|\zeta\|^2\right)\leq-\frac{\varepsilon}{2\delta_{max}^2}z^Tz-\frac{\varepsilon}{2}e^Te-\varepsilon z^T\left(\mathcal{H}^{-1}\otimes I\right)e \tag{17}$$

Using the relation that $-\varepsilon z^T\left(\mathcal{H}^{-1}\otimes I\right)e\leq\varepsilon\left(ke^T\left(\mathcal{H}^{-2}\otimes I_n\right)e+\frac{1}{k}z^Tz\right)\leq\varepsilon\left(k\frac{1}{\delta_{min}^2}e^Te+\frac{1}{k}z^Tz\right)$, (17) becomes

$$\delta^TS\delta\leq-\varepsilon\left(\|\varepsilon\|^2+\|\zeta\|^2\right)\leq\left(\frac{\varepsilon}{k}-\frac{\varepsilon}{2\delta_{max}^2}\right)z^Tz+\left(\frac{\varepsilon k}{\delta_{min}^2}-\frac{\varepsilon}{2}\right)e^Te,\quad k>0 \tag{18}$$

Substituting (18) into (15) yields

$$\dot{V}\leq\left(\frac{\varepsilon}{k}-\frac{\varepsilon}{2\delta_{max}^2}\right)z^Tz+\left(\frac{\varepsilon k}{\delta_{min}^2}-\frac{\varepsilon}{2}\right)e^Te+e^T\left(\frac{\mathcal{H}^2}{b_1}\otimes M_1^TM_1+\frac{\Theta^2}{b_2}\otimes M_2^TM_2\right)e$$

$$-2e^T(\Theta\otimes M_3-I_N\otimes M_1)z+2e^T(\Theta\otimes P_3A+\mathcal{H}\otimes M_1)e+e^T(\otimes P_3)e \tag{19}$$

Now the expression (19) consists only of accessible information e (measurement errors) and z (control inputs). In order to obtain a distributed rule, the last step is to diagonalize (19) by using the following two inequalities: $\mathcal{H}^2\leq\delta_{max}^2I$ and $e^T(\mathcal{H}\otimes M_1)e\leq\delta_{max}\|M_1\|e^Te$. Thus (19) becomes

$$\dot{V}\leq\sum_{i=1}^{N}\left(e_i^TQe_i+\Pi_1\|z_i\|^2+e_i^T\Pi_2z_i+\Pi_3\dot{\theta}_i\right) \tag{20}$$

where $\Pi_1=\frac{\varepsilon}{k}-\frac{\varepsilon}{2\delta_{max}^2}$, $\Pi_2=-2\theta_iM_3+2M_1$, $\Pi_3=e_i^TP_3e_i$, and Q is defined in (11)

Enforcing (20) being negative yields $\dot{\theta}_i(t)<\omega_i(t)$ with $\omega_i(t)$ defined in (10). One can also substitute (9) in (20) which yields $\dot{V}\leq-\sum_i\tau_i<0$. Therefore, the closed-loop system (7) is asymptotically stable, and the MAS (1) reaches leader-following consensus, which completes the proof.

LMI formulations

Notice that, in the above Theorem, the main difficulty lies in the determination of K and L_o, which involves a set of BMIs (8). In the following corollary, these BMIs are transferred to LMIs, which facilitate the numerical computation.

Corollary 1 (Wang and Chadli, 2024a) *The BMIs (8) in* **Theorem 1** *are satisfied if the following LMIs are satisfied with regard to* $P_1>0$, $P_2>0$, K *and* F:

$$\begin{cases}\Omega=\begin{pmatrix}I_N\otimes\mathrm{He}(P_1A)+I_{Nn}-2\dfrac{I_N\otimes P_1}{\mu_1} & 0_{Nn} & \mathcal{H}\otimes(P_1B) & \mu_1\mathcal{H}\otimes(K^TB^T)\\ * & \Omega_{22} & -I_N\otimes K^T & 0_{Nn}\\ * & * & -2I_{Nm} & 0_{Nm\times Nn}\\ * & * & * & -I_{Nn}\end{pmatrix}<0\\ \Omega_{22}=I_N\otimes\mathrm{He}(P_2A+FC)+(b_1+b_2)I_{Nn}\end{cases} \tag{21}$$

where b_1,b_2,μ_1 are arbitrary positive scalars. Then, the observer gain is obtained as $L_o=P_2^{-1}F$.

Proof. The proof is omitted but can be found in the article (Wang and Chadli, 2024a).

The presence of the positive term I_{Nn} in the first diagonal term of Ω (21) makes the result conservative. In the following corollary, another representation of LMIs with less conservatism is proposed.

Corollary 2 (Wang and Chadli, 2024a) *The BMIs (8) in* **Theorem 1** *are satisfied if the following conditions are satisfied:*

1. B has full column rank.
2. The following LMIs are satisfied with regard to $P_1>0$, $P_2>0$, N, R and F:

$$\begin{cases}\Xi=\begin{pmatrix}I_N\otimes\mathrm{He}(P_1A)-\mathcal{H}\otimes\mathrm{He}(BN) & -\mathcal{H}\otimes BN\\ * & I_N\otimes\mathrm{He}(P_2A+FC)+(b_1+b_2)I_{Nn}\end{pmatrix}<0\\ BR=P_1B\end{cases} \tag{22}$$

where b_1,b_2 are two arbitrary positive scalars. Then K,L_o are obtained as $K=R^{-1}N$, $L_o=P_2^{-1}F$.

Proof. One can first perform a change of variable of $F=P_2L_o$ in (8). If B has full column rank, then it follows from the linear matrix equality $BR=P_1B$ that R is also full rank, thus R is invertible which yields $B=P_1BR^{-1}$. Using the change of variable $N=RK$,

one can have

$$-\mathcal{H}\otimes \mathrm{He}(P_1BK) = -\mathcal{H}\otimes \mathrm{He}(BRK) = -\mathcal{H}\otimes \mathrm{He}(BN) \tag{23}$$

thus one can get Ξ, which completes the proof.

In Corollary 2, it is assumed that B has full column rank, implying that the dimension of the input is no more than the dimension of the state, i.e., $m\leq n$, and columns in B are linearly independent. This property exists in many autonomous systems such as quadrotor UAVs (Li and Li, 2011), VTOL aircraft (Chadli *et al.*, 2013), and autonomous ground vehicles (Hu *et al.*, 2016). Nevertheless, the matrix B should always be carefully examined, especially when dealing with over-actuated systems such as octorotor UAVs (Osmic *et al.*, 2016). In this case, the assumption of $m\leq n$ might be violated, and the Corollary 2 is not applicable.

Minimum inter-event time analysis

In the following result, an explicit expression of MIET is deduced, and it is proved that the Zeno behavior is excluded under **Theorem (1)**.

Corollary 3 (Wang and Chadli, 2024a) *Under* **Theorem 1**, *the inter-event time of agent i is lower-bounded by* t^i_{min} defined as

$$t^i_{min} = \int_0^{\bar{\theta}_i} \frac{\mathrm{d}h}{max(c_0 + c_1 h + c_2 h^2, 0) + \tau_i} \tag{24}$$

where $c_0 = \frac{1}{\eta}\left(\frac{\varepsilon k}{\delta^2_{min}} - \frac{\varepsilon}{2} + \frac{\varphi_1}{b_1} + 2\delta_{max}\rho_1 + \frac{\rho_1^2}{\sigma_1}\right)$, $c_1 = \frac{\alpha}{\eta}$, $c_2 = \frac{1}{\eta}(\frac{\varphi_2}{b_2} + \frac{\rho_3^2}{\sigma_2})$, $\alpha = \lambda_{max}(P_3A + A^TP_3)$, $\eta = \lambda_{min}(P_3)$, $\varphi_1 = \lambda_{max}(\mathcal{H}^2\otimes M_1^TM_1)$, $\varphi_2 = \lambda_{max}\ (M_2^TM_2)$, $\rho_1 = \|M_1\|$, $\rho_3 = \|M_3\|$, $k > 2\delta^2_{max}$, and σ_1, σ_2 are two positive scalars satisfying

$$\frac{\varepsilon}{2\delta^2_{max}} - \frac{\varepsilon}{k} - \sigma_1 - \sigma_2 = 0 \tag{25}$$

Proof. The proof is omitted but can be found in the article (Wang and Chadli, 2024a)

Through Corollary 3, t^i_{min} can be determined through numerical integration or analytical integration provided that $c_0 + c_1h + c_2h^2 \geq 0$, $h\in[0,\bar{\theta}_i]$. In the latter method, the analytical integration depends on the discriminant of $(c_0 + \tau_i) + c_1h + c_2h^2 = 0$, where its roots (could be complex numbers) are denoted as h_1 and h_2. Notice that c_0, c_1, c_2 are all positive and $(c_0 + \tau_i) + c_1h + c_2h^2 > 0$. In this case, t^i_{min} can be written in (26).

$$t^i_{min} = \begin{cases} \dfrac{1}{c_2(h_1-h_2)} ln\left(\dfrac{h_2(\bar{\theta}_i - h_1)}{h_1(\bar{\theta}_i - h_2)}\right), & \text{if} \Delta > 0 \\ -\dfrac{1}{c_2}\left(\dfrac{1}{h_1} + \dfrac{1}{\bar{\theta}_i - h_1}\right), & \text{if} \Delta = 0 \\ \dfrac{2}{\sqrt{-\Delta}}\left[arctan\left(\dfrac{2c_2\bar{\theta}_i + c_1}{\sqrt{-\Delta}}\right) - arctan\left(\dfrac{c_1}{\sqrt{-\Delta}}\right)\right], & \text{if} \Delta < 0 \end{cases} \tag{26}$$

where $\Delta = c_1^2 - 4(c_0 + \tau_i)c_2$.

Corollary 3 implies that the Zeno behavior of the proposed DETM is excluded. Notice that there is also a limitation of t^i_{min} when $\bar{\theta}_i$ approaches positive infinity. By adjusting the value of $\bar{\theta}_i$, one can vary the MIET and maintain the event frequency consistently lower than $1/t^i_{min}$. Increasing the value of $\bar{\theta}_i$ enables the inter-event time as long as possible not to overload the communication network. Indeed, a smaller $\bar{\theta}_i$ could also be designed to keep better surveillance and a higher convergence speed if the network allows it. Therefore, by choosing an appropriate parameter $\bar{\theta}_i$, the control performance and the communication frequency could achieve a good compromise.

According to the event-triggered strategy, the control performance in terms of convergence speed is not necessarily better than continuous control. Remember, the objective of the proposed method is to offer an advantage for systems that do not require high convergence speed, so the parameter $\bar{\theta}_i$ can be adjusted to minimize communication frequency. On the other hand, for systems that demand high convergence speed, the event frequency cannot be set too low. In summary, this method allows for a convenient adjustment of the balance between control performance and network usage as required.

Extension to Directed Topology

The aforementioned results could be extended to directed communication, where the representation topology is a digraph. Therefore, the following assumption for the digraph is adopted:

Assumption 4 *The graph* $\mathcal{G}$ *is fixed and directed. Furthermore, the augmented graph* $\overline{\mathcal{G}}$ contains a spanning tree with the leader agent being its root.

Recall the following property of matrix $\mathcal{H}$ due to Wang and Chadli (2023a) under Assumption 4:

Lemma 1 *Under* Assumption 4, *there exists a positive diagonal matrix* $\Psi = \mathrm{diag}(\psi_1, ..., \psi_N) > 0$ *such that* $\Psi\mathcal{H} + \mathcal{H}^T\Psi > 0$.

With the aid of matrix Ψ, the following theorem for designing DETM of MAS consensus under directed topology is proposed:

Theorem 2 (Wang and Chadli, 2023a) *The MAS described in (1) with directed topology will achieve leader-following consensus under the control law defined in (3) if there exist scalars $b_1>0$ and $b_2>0$*, matrices $P_1>0$, $P_2>0$, the controller gain K and the observer gain L_o satisfying the following inequality matrix:

$$S=\begin{pmatrix} \Psi\otimes \mathrm{He}(P_1A)-\mathrm{He}[(\Psi\mathcal{H})\otimes(P_1BK)] & -(\Psi\mathcal{H})\otimes(P_1BK) \\ * & \Psi\otimes\mathrm{He}(P_2A+P_2L_oC)+(b_1+b_2)I_{Nn} \end{pmatrix}<0 \tag{27}$$

and the matrix Ψ satisfying Lemma 1, with the event-triggered rule of agent i defined as

$$\begin{aligned} t^i_{k+1} &\triangleq inf\{t>t^i_k|\theta_i(t)\leq 0\}, \quad \theta_i(t^i_k)=\overline{\theta}_i \\ \dot{\theta}_i(t) &= \begin{cases} min(\omega_i(t),0)-\tau_i, & \text{if} \|e_i(t)\|\neq 0 \\ -\tau_i, & otherwise \end{cases} \end{aligned} \tag{28}$$

where $\overline{\theta}_i>0$, $\tau_i>0$, and $\omega_i(t)$ is defined as:

$$\omega_i(t)\triangleq -\frac{1}{\Pi_{3i}}\left[e_i^TQe_i+\varepsilon\left(\frac{1}{k}-\frac{\overline{\delta}_{min}}{2}\right)\|z_i\|^2+e_i^T(2\psi_iM_1-2\psi_i\theta_iM_3)z_i\right] \tag{29}$$

with $\Pi_{3i}=\psi_ie_i^TP_3e_i$, and

$$Q=\left(\varepsilon k\|\mathcal{H}^{-1}\|^2-\frac{\varepsilon}{2}+2\psi_{max}\|\mathcal{H}\|^2\|M_1\|\right)I_n+2\psi_i\theta_iP_3A+\frac{\psi_{max}\|\mathcal{H}\|^2}{b_1}M_1^TM_1+\frac{\psi_i^2\theta_i^2}{b_2}M_2^TM_2 \tag{30}$$

and $M_1=K^TB^TP_1$, $M_2=P_3L_oC$, $M_3=P_3BK$, $\psi_{max}=\|\Psi\|$, $\overline{\delta}_{min}=\lambda_{min}(\mathcal{H}^{-T}\mathcal{H}^{-1})$, $k>2/\overline{\delta}_{min}$, $P_3>0$. $\varepsilon>0$ is a scalar satisfying $S+\varepsilon I\leq 0$.

Proof. The proof follows a similar procedure of **Theorem 1** by replacing the matrix $\mathcal{H}$ as $\Psi\mathcal{H}$ and using a different Lyapunov function. The rest of the proof is omitted but can be found in Wang and Chadli (2023a).

Similar to the previous section, an LMI formalization of **Theorem 2** is presented in the following result.

Corollary 4 (Wang and Chadli, 2023a) *The design conditions (27) of* **Theorem 2** *are satisfied if there exist $P_1>0$, $P_2>0$, K and F* satisfying the following LMIs conditions:

$$\Omega=\begin{pmatrix} \Psi\otimes\mathrm{He}(P_1A)+I_{Nn}-2\frac{I_N\otimes P_1}{\mu_1} & 0_{Nn} & (\Psi\mathcal{H})\otimes(P_1B) & \frac{I_N\otimes P_1}{\mu_1}-\mu_1(\Psi\mathcal{H})\otimes(K^TB^T) \\ * & \Omega_{22} & -I_N\otimes K^T & 0_{Nn} \\ * & * & -2I_{Nm} & 0_{Nm\bar{n}Nn} \\ * & * & * & -I_{Nn} \end{pmatrix}<0 \tag{31}$$

where $\Omega_{22}=\Psi\otimes\mathrm{He}(P_2A+FC)+(b_1+b_2)I_{Nn}$, $b_1>0$, $b_2>0$, and $\mu_1>0$ are arbitrary positive scalars. Then, the observer gain is obtained as $L_o=P_2^{-1}F$.

Proof. The proof is omitted but can be found in Wang and Chadli (2023a).

If B has full column rank, one can formulate another LMI condition by the following corollary:

Corollary 5 (Wang and Chadli, 2023a) *The design conditions (27) of* **Theorem 2** *are satisfied if the following conditions are satisfied:*

1. B has full column rank.
2. The following LMIs are satisfied with regard to $P_1>0$, $P_2>0$, N, R and F:

$$\begin{cases} \Xi=\begin{pmatrix} \Psi\otimes\mathrm{He}(P_1A)-\mathrm{He}[(\Psi\mathcal{H})\otimes(BN)] & -(\Psi\mathcal{H})\otimes(BN) \\ * & \Psi\otimes\mathrm{He}(P_2A+FC)+(b_1+b_2)I_{Nn} \end{pmatrix}<0 \\ BR=P_1B \end{cases} \tag{32}$$

where b_1, b_2 are two arbitrary positive scalars. Then K, L_o are obtained as $K=R^{-1}N$, $L_o=P_2^{-1}F$.

Proof. The proof is quite similar to that of Corollary 2. One can first perform the change of variable of $F=P_2L_o$ in (27) thus the term S_{22} in S (8) becomes Ξ_{22}. If B has full column rank, then it follows that

$$-\mathrm{He}[(\Psi\mathcal{H})\otimes(P_1BK)]=-\mathrm{He}[(\Psi\mathcal{H})\otimes(BRK)]=-\mathrm{He}[(\Psi\mathcal{H})\otimes(BN)] \tag{33}$$

thus one can get Ξ, which completes the proof.

The following corollary deduces an explicit MIET and proves that the Zeno behavior does not exist under **Theorem 2**.

Corollary 6 (Wang and Chadli, 2023a) *Under* **Theorem 2**, *the inter-event time of agent i is lower-bounded by t^i_{min}* defined as

$$t^i_{min}=\int_0^{\overline{\theta}_i}\frac{\mathrm{d}h}{max(c_0+c_1h+c_2h^2,0)+\tau_i} \tag{34}$$

where

$$\begin{cases} c_0 = \left(\varepsilon k\|\mathcal{H}^{-1}\|^2 - \dfrac{\varepsilon}{2} + \dfrac{\psi_{max}\|\mathcal{H}\|^2\|M_1\|^2}{b_1} + 2\psi_{max}\|\mathcal{H}\|\|M_1\| + \dfrac{\psi_i\|M_1\|^2}{\sigma_1}\right)\dfrac{1}{\psi_i\eta} \\ c_1 = \dfrac{\alpha}{\eta}, c_2 = \dfrac{1}{\eta}\left(\dfrac{\psi_i\|M_2\|^2}{b_2} + \dfrac{\|M_3\|^2}{\sigma_2}\right), \alpha = \lambda_{max}\left(P_3A + A^TP_3\right), \quad \eta = \lambda_{min}(P_3) \end{cases} \tag{35}$$

with M_1, M_2, M_3 defined in **Theorem 2**, $k > 2/\bar{\delta}_{min}$, and σ_1, σ_2 are two positive scalars satisfying $\frac{\varepsilon\bar{\delta}_{min}}{2} - \frac{\varepsilon}{k} - \psi_i(\sigma_1 + \sigma_2) = 0$.

Proof. The proof can be found in Wang and Chadli (2023a).

Similar to Corollary 3, an analytical solution could be found through (26).

Numerical Example

In this section, an illustrative example is presented to validate the theoretical results. Consider a MAS with four follower agents and one leader. The system dynamics are defined in (1) with the following matrices, which can be found in Trejo *et al.* (2022).

$$A = \begin{pmatrix} -0.05 & 1 & 0 & 0 \\ -1 & 0 & 0 & 0 \\ 0 & 0 & 0 & 3 \\ 0 & 0 & -3 & 0 \end{pmatrix}, B = \begin{pmatrix} 1 & 0 \\ 1 & 0 \\ 0 & 1 \\ -1 & -1 \end{pmatrix}, C = \begin{pmatrix} 1 & 0 \\ 0 & 0 \\ 0 & 1 \\ 0 & 0 \end{pmatrix}^T \tag{36}$$

The agents' initial conditions are set as $x_0(0) = [-1 \;\; 1.5 \;\; 0.5 \;\; 1]^T$, $x_1(0) = [-2 \;\; 0 \;\; 0 \;\; 0]^T$, $x_2(0) = [0 \;\; 2 \;\; 0 \;\; 0]^T$, $x_3(0) = [0 \;\; 1 \;\; 0.1 \;\; 0]^T$, $x_4(0) = [2 \;\; 2 \;\; 0 \;\; 0]^T$. The initial states of observers are set as 0. Set $\bar{\theta}_i = 10, i = 1, ..., 4$. The communication topology is illustrated in **Fig. 2**. Notice that the leader agent is the root of the associated augmented graph $\bar{\mathcal{G}}$.

Since the matrix B has full column rank, **Theorem 1**, Corollary 1, and Corollary 2 are all available to calculate matrices K and L_o. Here, the Corollary 2 is applied with $b_1 = b_2 = 1$ and one can obtain the following solution in (37).

$$K = \begin{pmatrix} 0.0773 & 0.0722 & -0.0073 & -0.0911 \\ -0.0046 & -0.0018 & 0.0872 & -0.0903 \end{pmatrix}, L_o = \begin{pmatrix} -0.9888 & 1.0545 \\ -0.4478 & 0.4697 \\ -1.1269 & -1.3612 \\ -0.1063 & 0.3034 \end{pmatrix} \tag{37}$$

Fig. 3 illustrates the time evolution of consensus error. It can be seen that the system achieves the consensus among the agents. The consensus error asymptotically diminishes over time, indicating that the agents effectively coordinate their actions and align their states to

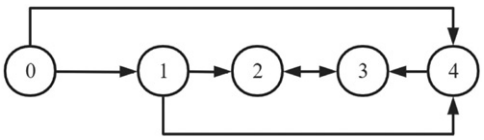

Fig. 2 The directed communication topology.

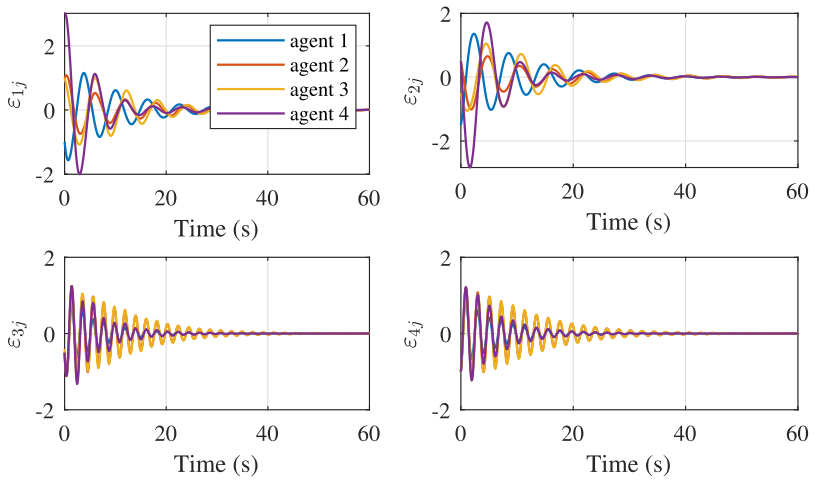

Fig. 3 Trajectory of consensus error of follower agents. ε_{ij} denotes the ith dimension of agent j's consensus error vector.

achieve a collective objective. This outcome validates the effectiveness of our control strategy in driving the system toward a desired consensus.

The observer state error in Fig. 4 demonstrates the convergence of the observer's estimated states to the actual states of the system. The diminishing observer state error signifies the accuracy and reliability of our observer design, which successfully tracks the true states of the system despite limited information availability. This highlights the practical significance of incorporating an observer in the control scheme, particularly in scenarios where direct state measurements are unattainable. Fig. 5 represents the control inputs corresponding to the proposed event-triggered control strategy.

The time evolution of the ADV $\theta_i(t)$ is presented in Fig. 6. It is evident that θ_i for each agent is asynchronous. This phenomenon arises due to the distributed nature of the MAS, where each agent operates independently based on its local information and interactions with neighboring agents. The events occur at the discontinuous points where θ_i is reset to $\overline{\theta}_i$, which shows a clock-like behavior.

Fig. 7 shows the evolution of the measurement error of each agent, where the discontinuous points imply events corresponding to those in Fig. 6.

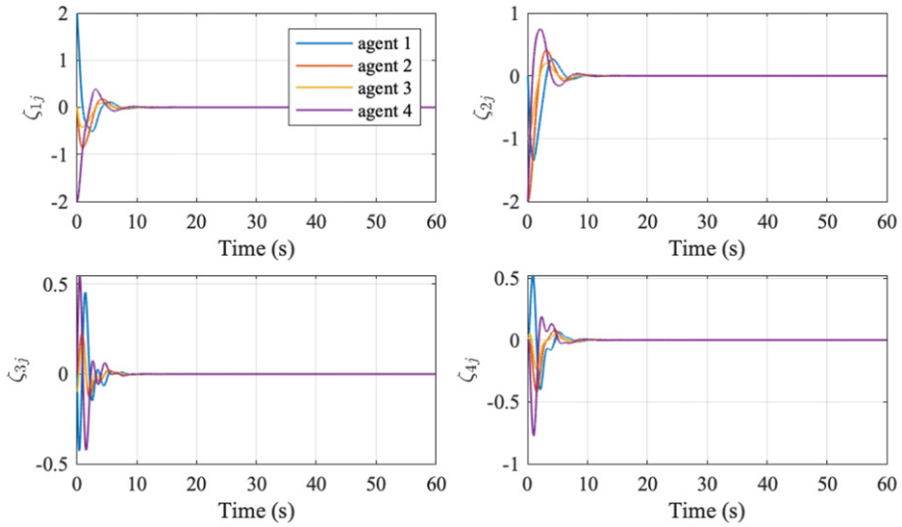

Fig. 4 Trajectory of observer state error of follower agents. ζ_{ij} denotes the ith dimension of agent j's observer state error vector.

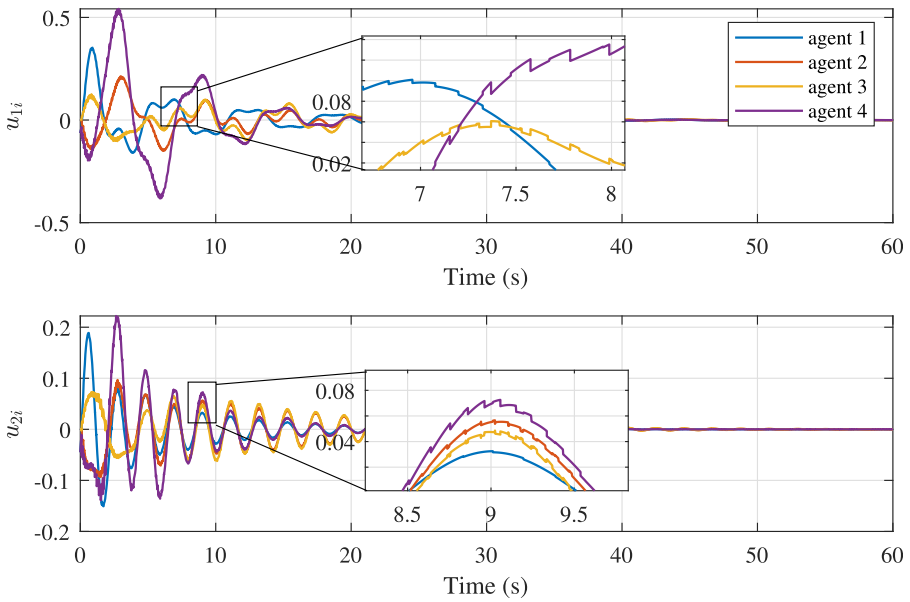

Fig. 5 Time evolution of control input of follower agents. u_{ji} denotes the jth dimension of agent i's control input vector.

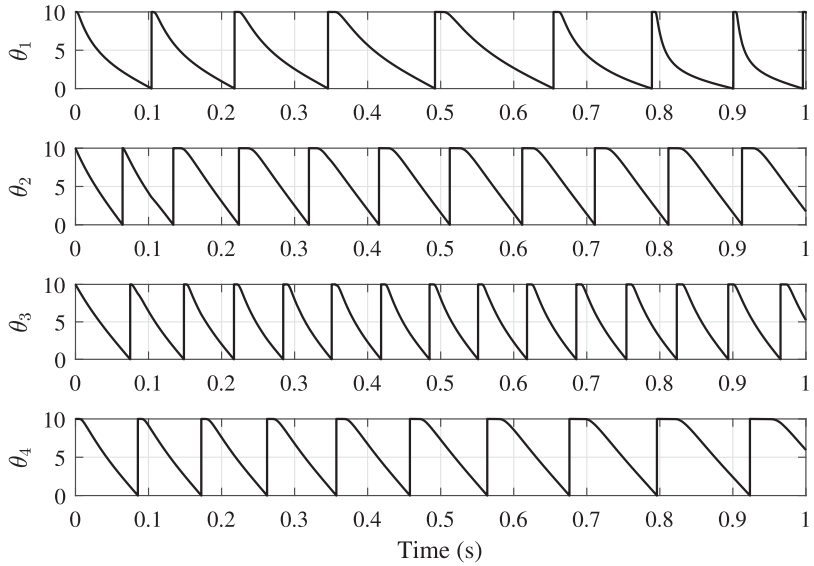

Fig. 6 Time evolution of auxiliary dynamic variables $\theta_i(t)$ of follower agents.

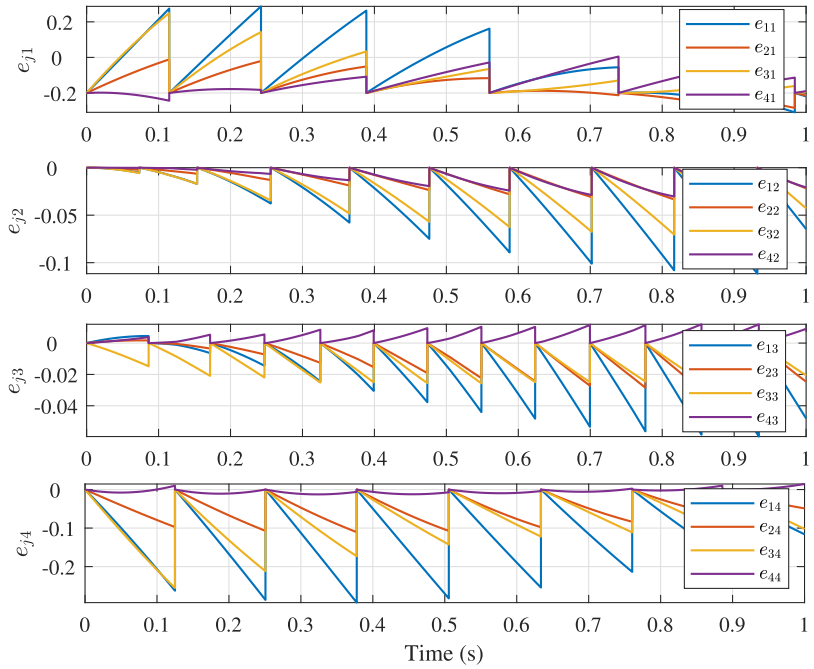

Fig. 7 Trajectory of measurement errorss of follower agents. e_{ji} denote the jth dimension of agent i's measurement error vector.

Furthermore, **Fig. 8** plots event-triggered instants for each agent within 60 s. The density of the event occurrence varies with time, which is much denser during the initial stage (initial 5 s) than when the system is stable (approximately after 45 s).

Additionally, **Fig. 9** plots t^i_{min} with different $\overline{\theta}_i$ using (34). The proposed DETM can prevent Zeno behavior as long as $\overline{\theta}_i > 0$. By adjusting $\overline{\theta}_i$, one can control the MIET and guarantee that the network communication is consistently below a designated frequency. Notice that t^i_{min} is only a lower bound of inter-event time and the actual inter-event time according to **Table1** is much longer than the MIET, which only serves as an indicator of the worst case.

Table 1 concludes the inter-event time using different event-triggered strategies: DETM from **Theorem 1**, the static event-triggered mechanism (SETM), and periodic communication with a fixed period of 0.001 s. For SETM, the Lyapunov function is the same as in the proof of **Theorem 1** by taking $\Theta = I_N; \Theta = 0$, which finally leads to a static event-triggered rule. According to this table, the inter-event time increases with larger $\overline{\theta}_i$ and can be easily tuned to be longer than SETM. For instance, the mean inter-event time under $\overline{\theta}_i = 500$ is 172.6 ms (5.8 Hz), while it is 1.105 ms (904 Hz) for the static approach and 1.000 ms (1000 Hz) for the fixed

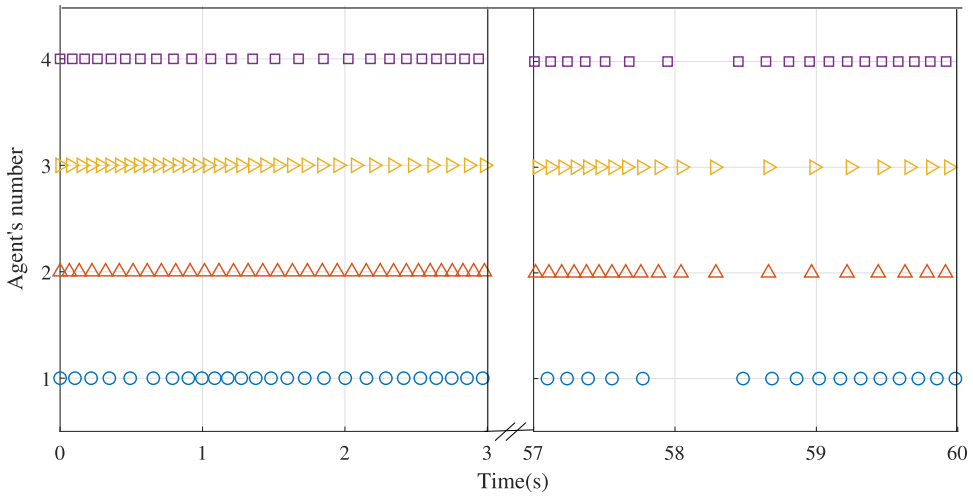

Fig. 8 Event-triggered instants of follower agents.

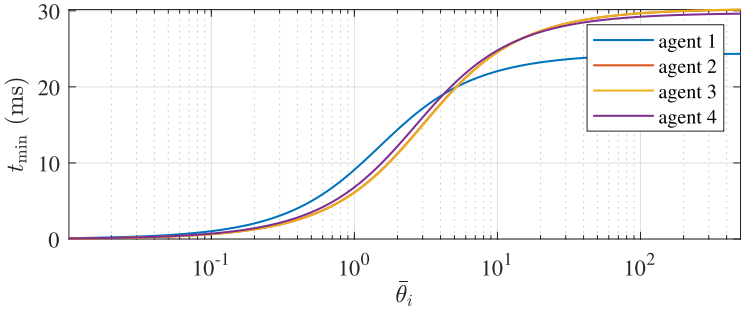

Fig. 9 Minimum inter-event time t^i_{min} with different θ_i using (24).

Table 1 Inter-event time (in ms) using different $\bar{\theta}_i$ under the proposed DETM (28), the SETM, and the periodic communication: mean values (Mean, i.e., the average event-triggered frequency), minimum values (Min, i.e., the agent with the highest event-triggered frequency) and maximum values (Max, i.e., the agent with the lowest event-triggered frequency) among five follower agents

Case	*DETM*					*SETM*	*Periodic*
	$\bar{\theta}_i = 0.1$	$\bar{\theta}_i = 1$	$\bar{\theta}_i = 10$	$\bar{\theta}_i = 100$	$\bar{\theta}_i = 500$		
Mean	76.09	113.1	165.2	172.5	172.6	1.105	1.000
Min	0.882	8.272	60.21	68.21	71.03	0.613	1.000
Max	101.1	617.3	709.3	680.2	684.8	3.565	1.000

period communication. Since the triggering frequency represents the usage of communication resources, in this scenario, one can save more than 99.36 and 99.42% of resource usage compared to the static strategy and to the fixed-period case, respectively.

Conclusion and Perspective

This chapter has introduced a design methodology for dynamical event-triggered controllers and observers for generic linear time-invariant multi-agent systems. The proposed solution aims to reduce the frequency of inter-agent information exchange by introducing a dynamic event-triggered protocol. This protocol allows for the convenient design of the inter-event time, and an explicit expression for the minimum inter-event time is presented, which enables more flexible tuning and prevents Zeno behavior. Both undirected and directed topologies are addressed under the leader-following scenario, and design conditions are formulated by linear matrix inequalities. Numerical examples have been illustrated. Simulation results indicate improvements in extending

the communication interval compared to periodic communication or static event-triggered methods, thus validating the efficacy of the proposed solution.

It is worth noting that the methodology outlined in this chapter offers a practical reference for linear multi-agent systems. However, it is important to recognize that several challenges persist, which are not fully addressed here. These challenges contain different perspectives, including but not limited to ETMs with easy-tunable parameters, ensuring performance guarantees for ETMs, and issues related to communication delay and unreliable network conditions, such as packet loss and cyberattacks. Interested readers are encouraged to consult the works of Nowzari *et al.* (2019) and Ge *et al.* (2021) for a more comprehensive study of these topics.

References

Berneburg, J., Nowzari, C., 2019. Distributed dynamic event-triggered coordination with a designable minimum inter-event time, in 2019 American Control Conference (ACC), pp. 1424-1429. ISSN: 2378-5861.

Borgers, D.P., Heemels, W.P.M.H., 2014. Event-separation properties of event-triggered control systems. IEEE Transactions on Automatic Control 59 (10), 2644-2656. Conference Name: IEEE Transactions on Automatic Control.

Chadli, M., Aouaouda, S., Karimi, H., Shi, P., 2013. Robust fault tolerant tracking controller design for a VTOL aircraft. Journal of the Franklin Institute 350 (9), 2627–2645

Cheng, B., Li, Z., 2019. Coordinated tracking control with asynchronous edge-based event-triggered communications. IEEE Transactions on Automatic Control 64 (10), 4321-4328. Conference Name: IEEE Transactions on Automatic Control.

Chen, X., Hao, F., 2015. Event-triggered consensus control of second-order multi-agent systems. Asian Journal of Control 17 (2), 592–603

Chu, X., Huang, N., Sun, Z., 2020. Event triggering control for dynamical systems with designable inter-event times. IFAC-PapersOnLine 53 (2), 6410–6415

Dimarogonas, D.V., Frazzoli, E., Johansson, K.H., 2012. Distributed event-triggered control for multi-agent systems. IEEE Transactions on Automatic Control 57 (5), 1291–1297

Donkers, M.C.F., Heemels, W.P.M.H., 2012. Output-based event-triggered control with guaranteed \cal L_infty-gain and improved and decentralized event-triggering. IEEE Transactions on Automatic Control 57 (6), 1362–1376. Conference Name: IEEE Transactions on Automatic Control.

Fan, Y., Feng, G., Wang, Y., Song, C., 2013. Distributed event-triggered control of multi-agent systems with combinational measurements. Automatica 49 (2), 671–675

Ge, X., Han, Q.-L., 2017. Distributed formation control of networked multi-agent systems using a dynamic event-triggered communication mechanism. IEEE Transactions on Industrial Electronics 64 (10), 8118–8127

Ge, X., Han, Q.-L., Zhang, X.-M., Ding, D., 2021. Dynamic event-triggered control and estimation: A survey. International Journal of Automation and Computing 18 (6), 857–886

Girard, A., 2015. Dynamic triggering mechanisms for event-triggered control. IEEE Transactions on Automatic Control 60 (7), 1992-1997. Conference Name: IEEE Transactions on Automatic Control.

Guo, H., Meng, M., Feng, G., 2023. Mean square leader-following consensus of heterogeneous multi-agent systems with Markovian switching topologies and communication delays. International Journal of Robust and Nonlinear Control 33 (1), 355–371. https://onlinelibrary.wiley.com/doi/pdf/10.1002/rnc.6456.

Gu, H., Liu, K., Zhu, G., Lü, J., 2023. Leader-following consensus of stochastic dynamical multi-agent systems with fixed and switching topologies under proportional-integral protocols. Asian Journal of Control 25 (2), 662–676. https://onlinelibrary.wiley.com/doi/pdf/10.1002/asjc.2897.

Hanada, K., Wada, T., Masubuchi, I., Asai, T., Fujisaki, Y., 2023. Multi-agent consensus with stopping rules under bounded measurement noise. Asian Journal of Control 25 (2), 651–661. https://onlinelibrary.wiley.com/doi/pdf/10.1002/asjc.2930.

Han, Q., Zhou, Y.-S., Tang, Y.-X., Tuo, X.-G., He, P., 2022. Event-triggered finite-time sliding mode control for leader-following second-order nonlinear multi-agent systems. IEEE Open Journal of Intelligent Transportation Systems 3, 570-579. Conference Name: IEEE Open Journal of Intelligent Transportation Systems.

Hou, Q., Dong, J., 2023. Robust adaptive event-triggered fault-tolerant consensus control of multiagent systems with a positive minimum interevent time. IEEE Transactions on Systems, Man, and Cybernetics: Systems 53 (7), 4003–4014

Hu, J., Geng, J., Zhu, H., 2015. An observer-based consensus tracking control and application to event-triggered tracking. Communications in Nonlinear Science and Numerical Simulation 20 (2), 559–570

Hu, C., Jing, H., Wang, R., Yan, F., Chadli, M., 2016. Robust H infinity output-feedback control for path following of autonomous ground vehicles. Mechanical Systems and Signal Processing 70 (71), 414–427

Liu, K.-Z., Teel, A.R., Sun, X.-M., Wang, X.-F., 2021. Model-based dynamic event-triggered control for systems with uncertainty: A hybrid system approach. IEEE Transactions on Automatic Control 66 (1), 444-451. Conference Name: IEEE Transactions on Automatic Control.

Li, J., Li, Y., 2011. Dynamic analysis and PID control for a quadrotor, in 2011 IEEE International Conference on Mechatronics and Automation, pp. 573-578. Beijing, China: IEEE.

Li, M., Long, Y., Li, T., Liang, H., Chen, C.L.P., 2023. Dynamic event-triggered consensus control for input constrained multi-agent systems with a designable minimum inter-event time. IEEE/CAA Journal of Automatica Sinica. 1–12

Li, X., Tang, Y., Karimi, H.R., 2020. Consensus of multi-agent systems via fully distributed event-triggered control',. Automatica 116, 108898.

Meng, X., Jiang, B., Karimi, H.R., Gao, C., 2023. Leader-follower sliding mode formation control of fractional-order multi-agent systems: A dynamic event-triggered mechanism. Neurocomputing 557, 126691.

Ni, W., Cheng, D., 2010. Leader-following consensus of multi-agent systems under fixed and switching topologies',. Systems & Control Letters 59 (3-4), 209–217

Nowzari, C., Garcia, E., Cortés, J., 2019. Event-triggered communication and control of networked systems for multi-agent consensus. Automatica 105, 1–27

Osmic, N., Kuric, M., Petrovic, I., 2016. Detailed octorotor modeling and PD control, in 2016 IEEE International Conference on Systems, Man, and Cybernetics (SMC), pp. 002182-002189. Budapest, Hungary: IEEE.

Pham, T.V., Nguyen, Q.T.T., 2023. Adaptive formation control of nonlinear multi-agent systems with dynamic event-triggered communication. Systems & Control Letters 181, 105652.

Qiu, A., Al-Dabbagh, A.W., Chen, T., 2019. A tradeoff approach for optimal event-triggered fault detection. IEEE Transactions on Industrial Electronics 66 (3), 2111-2121. Conference Name: IEEE Transactions on Industrial Electronics.

Qi, W., Zhang, C., Zong, G., Su, S.-F., Chadli, M., 2023. Finite-time event-triggered stabilization for discrete-time fuzzy markov jump singularly perturbed systems. IEEE Transactions on Cybernetics 53 (7), 4511-4520. Conference Name: IEEE Transactions on Cybernetics.

Ruan, X., Feng, J., Xu, C., Wang, J., 2020. Observer-based dynamic event-triggered strategies for leader-following consensus of multi-agent systems with disturbances. IEEE Transactions on Network Science and Engineering 7 (4), 3148–3158

Shi, J., 2021. Cooperative control for nonlinear multi-agent systems based on event-triggered scheme. IEEE Transactions on Circuits and Systems II: Express Briefs 68 (6), 1977–1981

Tabuada, P., 2007. Event-triggered real-time scheduling of stabilizing control tasks. IEEE Transactions on Automatic Control 52 (9), 1680-1685. Conference Name: IEEE Transactions on Automatic Control.

Trejo, J.A.V., Chadli, M., Rotondo, D., Medina, M.A., Theilliol, D., 2022. Event-triggered fault-tolerant leader-following control for homogeneous multi-agent systems. IFAC-PapersOnLine 55 (6), 79–84

Vazquez Trejo, J.A., Rotondo, D., Medina, M.A., Theilliol, D., 2020. Observer-based event-triggered model reference control for multi-agent systems, in 2020 International Conference on Unmanned Aircraft Systems (ICUAS), pp. 421-428. ISSN: 2575-7296.

Wang, Y., Cao, J., Wang, H., 2022. Event-based impulsive consensus for delayed multi-agent systems. Asian Journal of Control 24 (2), 771–781. https://onlinelibrary.wiley.com/doi/pdf/10.1002/asjc.2646.

Wang, Z., Chadli, M., 2023a. Distributed observer-based dynamic event-triggered control of multi-agent systems with adjustable inter-event time, in 2023 62nd IEEE Conference on Decision and Control (CDC), pp. 2391-2396. IEEE, Singapore, Singapore. ISSN: 2576-2370.

Wang, Z., Chadli, M., 2023b. Dynamic event-triggered control for multi-agent systems with adjustable inter-event time: a moving average approach, in Premier Congrès Annuel de la SAGIP, Marseille, France.

Wang, Z., Chadli, M., 2023c. Improved dynamic event-triggered consensus control for multi-agent systems with designable inter-event time, in 2023 31st Mediterranean Conference on Control and Automation (MED), pp. 818-823. Limassol, Cyprus: IEEE. ISSN: 2473-3504.

Wang, Z., Chadli, M., 2024a. Observer-based distributed dynamic event-triggered control of multi-agent systems with adjustable inter-event time (in presse). Asian Journal of Control.

Wang, Z., Chadli, M., 2024b, A virtual actuator and sensor approach for event-triggered fault-tolerant control of multi-agent systems (in presse), in 12th IFAC Symposium on Fault Detection, Supervision and Safety for Technical Processes (IFAC Safeprocess 2024). Ferrara, Italy: IEEE.

Wang, Z., Chadli, M., 2024c. Distributed joint fault estimation for multi-agent systems via dynamic event-triggered communication. IEEE Control Systems Letters 8, 868–873. In this issue.

Wen, G., Wang, P., Lv, Y., Chen, G., Zhou, J., 2023. Secure consensus of multi-agent systems under denial-of-service attacks. Asian Journal of Control 25 (2), 695–709. https://onlinelibrary.wiley.com/doi/pdf/10.1002/asjc.2953.

Wu, X., Mao, B., Wu, X., Lu, J., 2022. Dynamic event-triggered leader-follower consensus control for multiagent systems. SIAM Journal on Control and Optimization 60 (1), 189–209. (Society for Industrial and Applied Mathematics).

Wu, Z.-G., Xu, Y., Lu, R., Wu, Y., Huang, T., 2018. Event-triggered control for consensus of multiagent systems with fixed/switching topologies. IEEE Transactions on Systems, Man, and Cybernetics: Systems 48 (10), 1736-1746. Conference Name: IEEE Transactions on Systems, Man, and Cybernetics: Systems.

Wu, Y., Yang, X., Yan, H., Chadli, M., Wang, Y., 2023. Adaptive fuzzy event-triggered sliding-mode control for uncertain euler-lagrange systems with performance specifications. IEEE Transactions on Fuzzy Systems 31 (5), 1566-1579. Conference Name: IEEE Transactions on Fuzzy Systems.

Xu, W., He, W., Ho, D.W.C., Kurths, J., 2022. Fully distributed observer-based consensus protocol: Adaptive dynamic event-triggered schemes. Automatica 139, 110188.

Yang, R., Liu, L., Feng, G., 2022. Leader-following output consensus of heterogeneous uncertain linear multiagent systems with dynamic event-triggered strategy. IEEE Transactions on Systems, Man, and Cybernetics:Systems 52 (3), 1626–1637

Yang, D., Ren, W., Liu, X., Chen, W., 2016. Decentralized event-triggered consensus for linear multi-agent systems under general directed graphs. Automatica 69, 242–249

Yang, Y., Shen, B., Han, Q.-L., 2023. Dynamic event-triggered scaled consensus of multi-agent systems in reliable and unreliable networks. IEEE Transactions on Systems, Man, and Cybernetics: Systems. 1–13

Zhang, H., Feng, G., Yan, H., Chen, Q., 2014. Observer-based output feedback event-triggered control for consensus of multi-agent systems. IEEE Transactions on Industrial Electronics 61 (9), 4885–4894

Zhang, K., Zhou, B., Yang, X., Duan, G.-R., 2023. Time-varying event-triggered and self-triggered bounded control of linear systems with a designable minimal interevent time. IEEE Transactions on Systems, Man, and Cybernetics: Systems, pp. 1-11. Conference Name: IEEE Transactions on Systems, Man, and Cybernetics: Systems.

Zhu, G., Liu, K., Gu, H., Luo, W., Lu, J., 2022. Observer-based event-triggered formation control of multi-agent systems with switching directed topologies. IEEE Transactions on Circuits and Systems I: Regular Papers 69 (3), 1323–1332